

MODELING THE HOT DEFORMATION FLOW CURVES OF API X65 PIPELINE STEEL USING THE POWER LAW EQUATION

M. Rakhshkhorshid*

* rakhshkhorshid@birjandut.ac.ir

Received: November 2015

Accepted: August 2016

Department of Mechanical Engineering, Birjand University of Technology, Birjand, Iran.

Abstract: Till now, different constitutive models have been applied to model the hot deformation flow curves of different materials. In this research, the hot deformation flow stress of API X65 pipeline steel was modeled using the power law equation with strain dependent constants. The results was compared with the results of the other previously examined constitutive equations including the Arrhenius equation, the equation with the peak stress, peak strain and four constants and the equation developed based on a power function of Zener-Hollomon parameter and a third order polynomial function of strain power a constant number. Root mean square error (RMSE) criterion was used to assess the performance of the understudied models. It was observed that the power law equation with strain dependent constants has a better performance (lower RMSE) than that of the other understudied constitutive equations except for the equation with the peak stress, peak strain and four constants. The overall results can be used for the mathematical simulation of hot deformation processes.

Keywords: Constitutive Equations, Hot Deformation Processes, Power Law Equation, API X65 Pipeline Steel.

1. INTRODUCTION

API X65 pipeline steel is a high strength low alloy (HSLA) steel that is characterized by API (American petroleum Institute) standard code [1]. This steel is produced by thermo-mechanical processing (TMP) [2, 3]. For designation and optimization of the thermo-mechanical processing of a material, the response of it to the external loading should be determined. In the other words, the material behaviour at different deformation conditions (i.e. at different temperatures, strains and strain rates) should be characterized [4].

Till now, many different constitutive equations have been developed to model the hot deformation flow curves of different materials [5-8]. After determination of the material behavior (using a constitutive equation), finite element method (FEM) codes can be applied to simulate the thermomechanical processes [8-10]. The overall constitutive equations can be divided into three categories including the physical-based constitutive equations, the phenomenological constitutive equations and artificial neural network (ANN) models [11].

In physical-based constitutive models, the mechanisms of deformation such as dislocation

dynamics and thermal activation are considered. Zerilli-Armstrong [12] and a two-stage constitutive model [13] developed based on the classical stress-dislocation relation and the kinetics of dynamic recrystallization are the examples of physical-based models. Although, these models provide higher modeling performance than that of the phenomenological models, they have a larger number of constants and need to numerous

accurate experiments to extract the material constants [4].

On the other hand, phenomenological constitutive equations can be developed easily through the conducting some limited number of tests (such as hot torsion or hot compression tests). Till now, many efforts have been done to develop the new phenomenological constitutive equations. Johnson-Cook [5], Arrhenius type constitutive equation [14], a model with the peak stress, peak strain, and four constants developed by Mirzadeh and Najafzadeh [8] and a new simple model developed based on a power function of Zener-Hollomon parameter and a third order polynomial function of strain power a constant number [15] are some examples of phenomenological constitutive equations. The Arrhenius type constitutive equation is one of the

most famous phenomenological constitutive equations that have ever been used to model the hot deformation behavior of different materials [15-17]. For example, Badami et al. used this model to describe the hot compression behavior of an Al6061 aluminum alloy [16]. Also, this model has been applied to express the flow curves of 20CrMo alloy steel by He et al. [17].

Because of the nonlinear and sophisticated behavior of materials at elevated temperatures, artificial neural network models has largely been used to model the hot flow curves of different materials [18-22]. For example, Lin et al. developed an artificial neural network model to investigate the effects of deformation temperature, strain rate and strain on the flow behavior of 42CrMo steel [19]. Also, a three-layer feed-forward ANN with a back-propagation learning algorithm has been developed by Mandal et al. to predict the flow behavior of austenitic stainless steels at hot deformation condition [22].

However, according to the literature survey, the power law equation has not been yet used to model the flow curves of API X65 pipeline steel. Arrhenius equation with strain dependent constants, an equation with the peak stress, peak strain and four constants and a new simple model developed based on a power function of Zener-Hollomon parameter and a third order polynomial function of strain power a constant number are the models that has ever been used to model the hot deformation flow curves of tested steel [15]. In this study, the power law equation with strain dependent constants is used to model the hot deformation flow curves of tested steel. The results are compared with the results of the other previously examined equations.

2. THE EXPERIMENTAL FLOW CURVES

The results of single hit compression tests conducted at elevated temperatures were used to develop the constitutive equations [23]. The compression tests were conducted on a 250 kN Zwick tensile/compression testing machine equipped with a radiant furnace. More details about the conducted compression tests have been reported in Ref. [23]. The chemical composition of tested steel is presented in table 1. Experimental flow curves of API X65 pipeline steel, obtained at deformation conditions with the temperatures of 900, 950, 1000, 1050, 1100 and 1150 °C with the different strain rates of 0.01, 0.1, and 1 s⁻¹ for each of the deformation temperatures are shown in Fig. 1 [23]. The shape of the true stress–true strain curves obtained at different deformation conditions is the result of the competition between the work hardening and the work softening mechanisms. As can be seen in most deformation conditions, the flow stress increases to a peak value and then gradually falls to a steady state stress that is the common pattern of dynamic recrystallization (DRX) occurrence. Though, for the most severe deformation condition with the temperature of 950 °C and the strain rate of 1 s⁻¹, true stress–true strain curve shows a typical dynamic recovery (DRV) behavior [23].

3. RESULTS AND DISCUSSION

In this section, the power law equation with strain dependent constants is applied to model the hot deformation flow curves of API X65 pipeline steel. Furthermore, the results of this constitutive equation are compared with the results of a model has recently been developed based on a power function of Zener-Hollomon parameter and a

Table 1. The chemical composition of API X65 steel (all in wt%) [21].

C	Si	Mn	P	S	Cr	Mo	Ni	Al	Cu	V	Ti	Nb
0.072	0.201	1.450	0.008	0.002	0.174	0.240	0.009	0.023	0.008	0.050	0.015	0.047

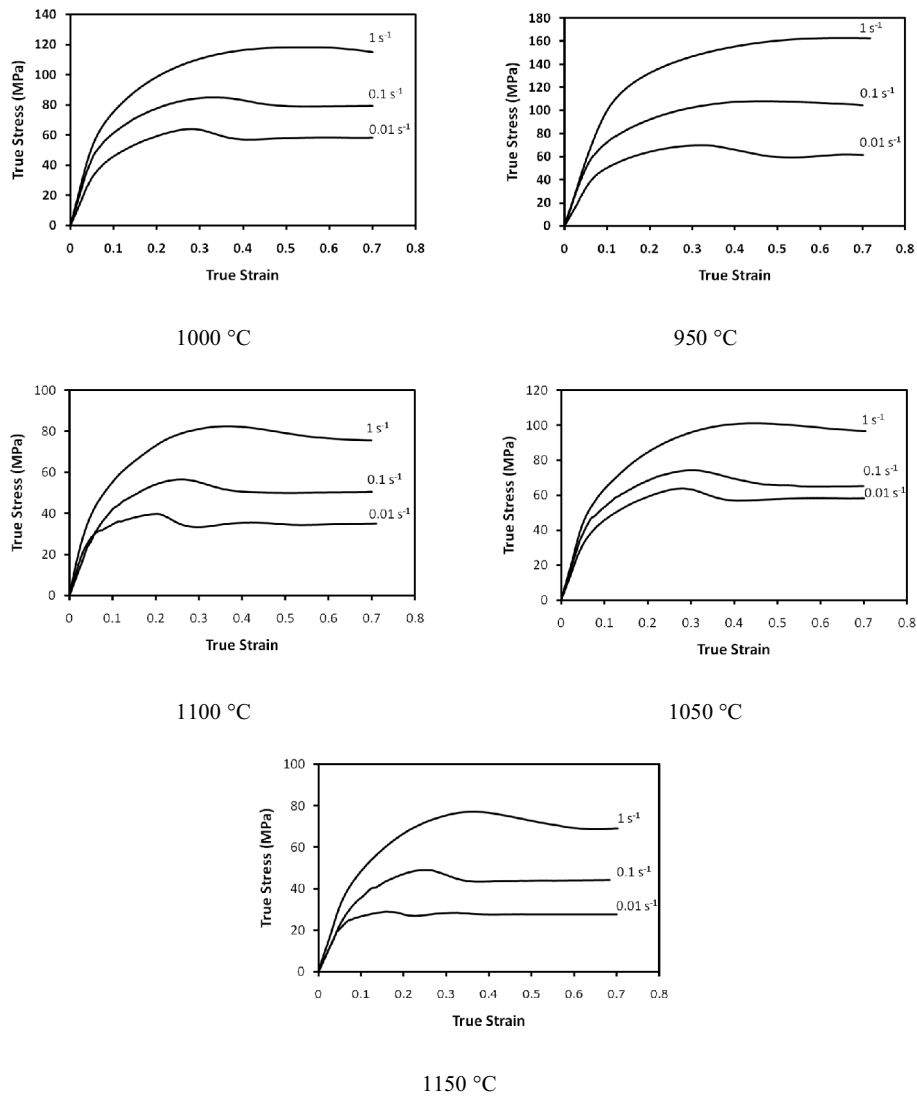


Fig. 1. Experimental flow curves of API X65 pipeline steel at different temperatures and strain rates [21].

third order polynomial function of strain power m (m is a constant) [15].

3. 1. Power Law Equation with Strain Dependent Constants

To describe the flow stress of different materials at hot deformation conditions, it is needed to deal with the effects of temperature and strain rate on the flow curves as well as the effect of the strain. Usage of the equations in which the Zener–Hollomon parameter (Z) is considered as a

function of stress is a common practice for this purpose [23]:

$$Z = \dot{\epsilon} \exp\left(\frac{Q}{RT}\right) = f(\sigma) \quad (1)$$

where Q is the activation energy (J/mol), R is the universal gas constant and T is the absolute temperature. Substituting the power law equation as the $f(\sigma)$ in Eq. 1, gives:

$$Z = f(\sigma) = A' \sigma^{n'} \quad (2)$$

where A' and n' are material constants. The Eq. 2 should be rewritten for a characteristic stress or a stress corresponding to a certain strain (for example for the stress corresponding to the strain of 0.3). Usually, these equations are derived for the peak stress [23, 24]. However, for flow stress modeling, it is suggested that the constants of the constitutive equations should be expressed as polynomial functions of strain to compensate the effect of strain [4, 11, 23]. Here, to derive the power law equation, for the tested steel, Eq. 2 was rewritten for the stresses corresponding to the strains in the range of 0.1 to 0.7 with step size of 0.05, at the first. Then, the regression analysis was used to fit polynomial functions over the obtained constants for different strains. A more detailed discussion has been provided as in the follow.

Substituting $f(\sigma)$ from Eq. 2 in Eq. 1 and taking the natural logarithm, yields:

$$\ln \dot{\epsilon} + \frac{Q}{R} \left(\frac{1}{T} \right) = \ln A' + n' \ln \sigma \quad (3)$$

The partial differentiation of Eq. (3) can be written as:

$$\partial \ln \dot{\epsilon} + \frac{Q}{R} \partial \left(\frac{1}{T} \right) = n' \partial \ln \sigma \quad (4)$$

The temperature constant condition in Eq. (4) gives:

$$n' = \left. \frac{\partial \ln \dot{\epsilon}}{\partial \ln \sigma} \right|_T \quad (5)$$

Similarly, the $\dot{\epsilon}'$ constant condition in Eq. (4) gives:

$$Q = R n' \left. \frac{\partial \ln \sigma}{\partial \left(\frac{1}{T} \right)} \right|_{\dot{\epsilon}} \quad (6)$$

According to the Eqs. (5) and (6) the plots of $\ln \dot{\epsilon} - \ln \sigma$ and $\ln \sigma - 1/T$ (for stresses corresponding to different strains) can be used to calculate the n' and Q constant values, respectively. Diagrams of $\ln \dot{\epsilon} - \ln \sigma$ plotted for the stresses corresponding to the strain of 0.3 (extracted from the fifteen experimental flow curves with different temperatures and strain rates) are depicted in Fig. 2.

As presented in Fig. 2, the average value of n' has been calculated equal to 5.996. Moreover, diagrams of $\ln \sigma - 1/T$ plotted for the stresses corresponding to the strain of 0.3 (extracted from the fifteen experimental flow curves with different temperatures and strain rates) are depicted in Fig. 3.

As presented in Fig. 3, the average slope value

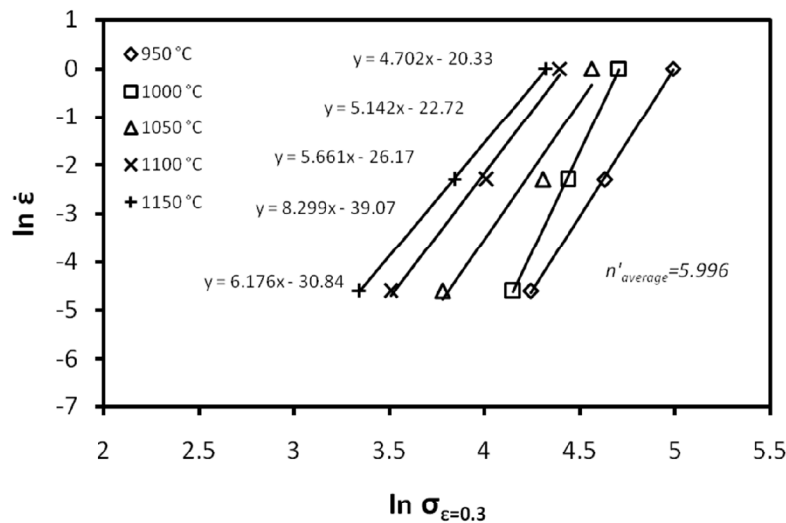


Fig. 2. Diagrams of $\ln \dot{\epsilon} - \ln \sigma$ plotted to calculate the average value of n'

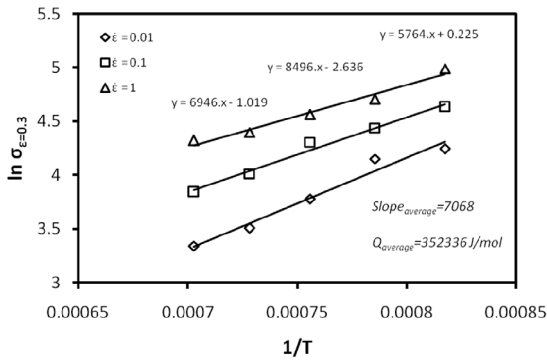


Fig. 3. Diagrams of $\ln\sigma-1/T$ plotted to calculate the average value of Q

has been calculated equal to 7068. According to Eq. 6, the average slope value obtained from $\ln\sigma-1/T$, should be multiplied by Rn' to calculate the value of Q . As depicted in Fig. 3, the value of Q for the stresses corresponding to the strain of 0.3 has been calculated equal to 352336 J/mol. Substituting the values of n' and Q in Eq. 3 and rewriting this equation for different deformation conditions (i.e. different temperatures and strain rates), the value of $\ln A'$, using a Newtonian optimization method, has been calculated equal to 4.55. Similarly, the values of n' , Q and $\ln A'$ for the stresses corresponding to the strains in the range of 0.1 to 0.7 with step the size of 0.05 are calculated. The overall results are presented in Fig. 4.

As depicted in Fig. 4, the regression analysis was used to express the constants of the power law equation as polynomial functions of the strain. The results are summarized as follows:

$$n' = -10.98\varepsilon^3 + 30.39\varepsilon^2 - 22.56\varepsilon + 10.35 \quad (7)$$

$$Q = 528,675\varepsilon^2 - 519,309\varepsilon + 456,116 \quad (8)$$

$$\ln A' = 7.672\varepsilon^3 - 19.96\varepsilon^2 + 18.82\varepsilon + 0.001 \quad (9)$$

Substituting the materials constants as the functions strain, the following equation (derived from Eq. 3) was used to model the flow stress:

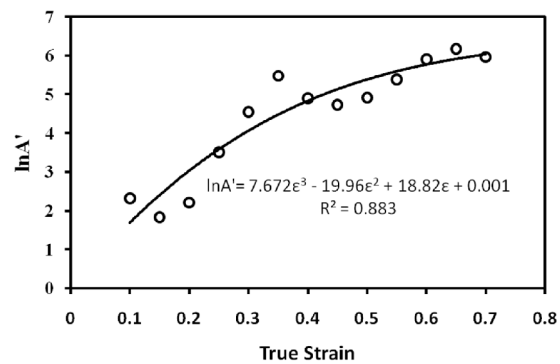
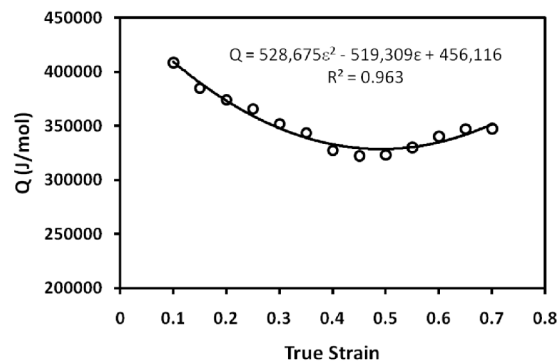
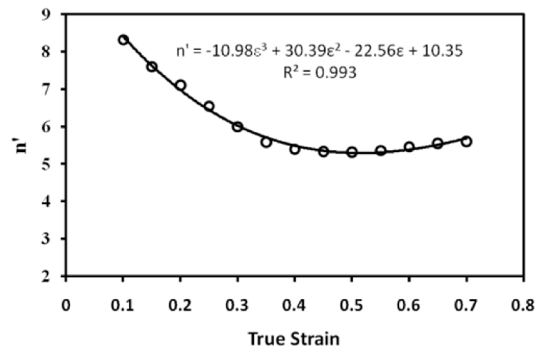


Fig. 4. The values of n' , Q and $\ln A'$ calculated for the stresses corresponding to the strains in the range of 0.1 to 0.7.

$$\sigma = \left[\dot{\varepsilon} \exp\left(\frac{Q}{RT}\right) / A' \right]^{\frac{1}{n'}} \quad (10)$$

A comparison between the experimental and modeled flow curves (using the power law constitutive equation), at deformation conditions with two temperatures of 1000 and 1100 °C with

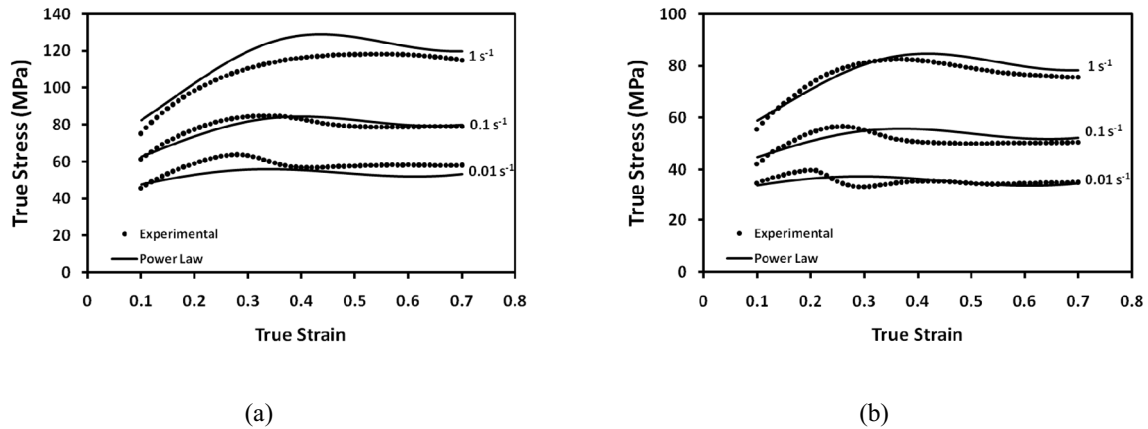


Fig. 5. The comparison between the experimental and modeled flow curves (using the power law constitutive equation) at deformation conditions with two temperatures of (a) 1000 and (b) 1100 °C with different strain rates.

different strain rates, are presented in Figs. 5(a) and 5(b), respectively.

3. 2. The other Previously Examined Constitutive Equations

In this section, the results of the other previously examined constitutive equations including the Arrhenius equation, the equation with the peak stress, peak strain, and four constants and The equation developed based on a power function of Zener-Hollomon parameter and a third order polynomial function of strain power a constant number (from the Ref. [15]) for flow stress modeling of API X65 pipeline steel are presented to compare with the results of the power law equation.

3. 2. 1. Arrhenius Equation

As explained in Ref. [15], using the Arrhenius equation with strain dependent constants the hot flow stress of API X65 pipeline steel has been obtained as follows:

$$\sigma = \frac{1}{\alpha} \ln \left\{ (Z/A)^{1/n} + [(Z/A)^{2/n} + 1]^{1/2} \right\} \quad (11)$$

where strain dependent constants of the equation above can be expressed by the following equations:

$$\alpha = 0.243\varepsilon^4 - 0.526\varepsilon^3 + 0.413\varepsilon^2 - 0.136\varepsilon + 0.030 \quad (12)$$

$$n = 12.915\varepsilon^2 - 13.556\varepsilon + 7.403 \quad (13)$$

$$Q = -3731.9\varepsilon^4 + 5459.1\varepsilon^3 - 1965.9\varepsilon^2 - 141.0\varepsilon + 451.9 \quad (14)$$

$$\ln A = -381.159\varepsilon^4 + 579.768\varepsilon^3 - 239.617\varepsilon^2 + 5.911\varepsilon + 36.087 \quad (15)$$

More details about finding the constants of the Arrhenius equation for the tested steel can be found in Ref. [15].

3. 2. 2. The Equation with the Peak Stress, Peak Strain, and Four Constants

This equation has been developed firstly by Mirzadeh and Najafizadeh [8] and it was used to model the hot deformation flow curves 17-4 PH stainless steel. This equation has been used by the author to model the hot flow stress of API X65 pipeline steel [15]:

$$\sigma = \sigma_p \times \left(-1.32 + 5.90 \left(\frac{\varepsilon}{\varepsilon_p} \right)^{0.4} - 4.93 \left(\frac{\varepsilon}{\varepsilon_p} \right)^{0.8} + 1.32 \left(\frac{\varepsilon}{\varepsilon_p} \right)^{1.2} \right) \quad (16)$$

where, in the equation above the values of σ_p and ε_p are the peak stress and peak strain and can be obtained through the following relations from the previous work of the authors [15]:

$$\sigma_p = 0.576 \times Z^{0.173} \quad (17)$$

$$\varepsilon_p = 0.0045 \times Z^{0.153} \quad (18)$$

More details about finding the constants of this equation for the tested steel can be found in Ref. [15].

3. 2. 3. The Equation Developed Based on a Power Function of Zener-Hollomon Parameter and a Third Order Polynomial Function of Strain Power a Constant Number

This equation has been developed by the author [15] and was used to describe the hot deformation flow curves of API X65 pipeline steel. As explained in Ref. [15] using the equation developed based on a power function of Zener-Hollomon parameter and a third order polynomial function of strain power a constant number the hot flow stress of API X65 pipeline steel can be expressed as follows [15]:

$$\sigma = \dot{\varepsilon}^{0.169} \exp \left(\frac{0.169 \times 346238}{RT} \right) \times (-0.006 + 2.420\varepsilon^{0.7} - 3.899\varepsilon^{1.4} + 2.046\varepsilon^{2.1}) \quad (19)$$

More details about finding the constants of this equation for the tested steel can be found in Ref. [15].

3. 3. Comparison of the Results of Power Law Equation with the other Constitutive Equations

The root mean square error (RMSE) criterion was used to assess and compare the modeling performance of understudied constitutive equations:

$$RMSE = \sqrt{\frac{1}{n} \sum_{i=1}^n (t_i - y_i)^2} \quad (20)$$

where t_i is the target output, y_i is the model output and n is the number of overall data patterns. The RMSE value obtained for the power law is compared with the other previously examined equations for the tested steel in table 2.

As presented in table 2, the power law equation with strain dependent constants has a better performance than that of the other examined equations, except for the equation with the peak stress, peak strain, and four constants.

Table 2. Root mean square error (MPa) obtained for the understudied equations.

Constitutive equation	Root Mean Square Error (MPa)
Arrhenius equation with strain dependent constants [15]	5.48
Constitutive equation with the peak stress, peak strain, and four constants [15]	3.64
The model developed based on a power function of Zener-Hollomon parameter and a third order polynomial function of strain power a constant number [15]	4.74
Power law equation with strain dependent constants	4.12

4. CONCLUSION

In this research, the power law equation with strain dependent constants was used to model the hot flow curves of API X65 pipeline steel. The results of this model was compared with the results of the other previously examined constitutive equations including the Arrhenius equation, the equation with the peak stress, peak strain and four constants and the equation developed based on a power function of Zener-Hollomon parameter and a third order polynomial function of strain power a constant number. The overall results can be summarized as follows:

1. Using the power law equation with strain dependent constants the hot deformation flow stress of API X65 can be obtained through the following equation:

$$\sigma = \left[\dot{\varepsilon} \exp\left(\frac{Q}{RT}\right) / A' \right]^{\frac{1}{n'}}$$

where, strain dependent constants of the equation above can be expressed by the following equations:

$$\begin{aligned} n' &= -10.98 \varepsilon^3 + 30.39 \varepsilon^2 - 22.56 \varepsilon + 10.35 \\ Q &= 528,675 \varepsilon^2 - 519,309 \varepsilon + 456,116 \\ \ln A' &= 7.672 \varepsilon^3 - 19.96 \varepsilon^2 + 18.82 \varepsilon + 0.001 \end{aligned}$$

2. Using the RMSE criterion, it was found that the power law equation with strain dependent constants has a lower RMSE than that of the other understudied constitutive equations except for the equation with the peak stress, peak strain, and four constants.

5. ACKNOWLEDGEMENT

The author gratefully acknowledges the financial support from the Birjand University of Technology under the grant number RP/94/1001.

REFERENCES

1. API Specifications 5L, Specifications for LinePipe, 44th Edition, American Petroleum Institute, USA, 2007.
2. Rakhshkhorshid, M and Hashemi, S. H., "Firefly algorithm assisted optimized NN to predict the elongation of API X65 pipeline steel", *IJMMNO*, 2013, 4(3), 238-251.
3. Hashemi, S. H. and Mohammadyani, D., "Characterisation of weldment hardness, impact energy and microstructure in API X65 steel", *Int. J. Pres. Ves. Pip.*, 98, 2012, 8-15.
4. Abbasi-Bani, A., Zarei-Hanzaki, A., Pishbin, M. H. and Haghdadi, N., "A comparative study on the capability of Johnson-Cook and Arrhenius-type constitutive equations to describe the flow behavior of Mg-6Al-1Zn alloy", *Mech. Mater.*, 71, 2014, 52-61.
5. Johnson, G. R. and Cook, W. H., "A constitutive model and data for metals subjected to large strains, high strain rates and high temperatures, In Proceedings of the 7th international symposium on ballistics", 1983, 541-543.
6. Voce, E., The relationship between stress and strain for homogeneous deformation, *J. Inst. Metals.*, 74, 1948, 537-562.
7. Khan, A. S. and Huang, S., "Experimental and theoretical study of mechanical behavior of 1100 aluminum in the strain rate range 10⁻⁵-104 s⁻¹", *Int. J. Plasticity*, 8, 1992, 397-424.
8. Mirzadeh, H. and Najafizadeh, A., "Flow stress prediction at hot working conditions", *Mater. Sci. Eng., A* 527, 2010, 1160-1164.
9. Peng, K., Zhong, H., Zhao, L., Xue K., and Ji, Y., "Strip shape modeling and its setup strategy in hot strip mill process", *Int. J. Adv. Manuf. Technol.*, 72, 2014, 589-605.
10. Zhan, M. Y., Chen, Z., Zhang, H. and Xia, W., "Flow stress behavior of porous FVS0812 aluminum alloy during hot-compression", *Mech. Res. Commun.*, 33, 2006, 508-514.
11. Lin, Y. C. and Chen, X. M., "A critical review of experimental results and constitutive descriptions for metals and alloys in hot working", *Mater. Design*, 32, 2011, 1733-1759.
12. Zerilli, P. J. and Armstrong, R. W., "Dislocation-mechanics-based constitutive

- relations for material dynamics calculations”, *J. Appl. Phys.*, 61, 1987, 1816–1825.
13. Lin, Y. C., Chen, M. S. and Zhang, J., “Prediction of 42CrMo steel flow stress at high temperature and strain rate”, *Mech. Res. Commun*, 35, 2008, 142–150.
 14. Shi, H., McLaren, A. J., Sellars, C. M., Shahani, R. and Bolingbroke, R., “Constitutive equations for high temperature flow stress of aluminum alloys”, *J. Mater. Sci. Technol.*, 13, 1997, 210–216.
 15. Rakhshkhorshid, M., “Modeling the hot deformation flow curves of API X65 pipeline steel”, *Int. J. Adv. Manuf. Technol.*, 77, 2015, 203–210.
 16. Badami, E., Salehi, M. T. and Seyedein, S. H., “Modeling high temperature flow behavior of an Al6061 aluminium alloy”, *Iranian Journal of Materials science and engineering*, 11(4), 2014, 63-71.
 17. He, A., Xie, G., Zhang, H. and Wang, X., “A comparative study on Johnson–Cook, modified Johnson–Cook and Arrhenius-type constitutive models to predict the high temperature flow stress in 20CrMo alloy steel”, *Mater. Design*, 52, 2013, 677–685.
 18. Haghdam, N., Zarei-Hanzaki, A., Khalesian, A. R. and Abedi, H. R., “Artificial neural network modeling to predict the hot deformation behavior of an A356 aluminum alloy”, *Mater. Design*, 49, 2013, 386-391.
 19. Lin, Y. C., Zhang, J. and Zhong, J., “Application of neural networks to predict the elevated temperature flow behavior of a low alloy steel”, *Comput. Mater. Sci.*, 43, 2008, 752-758.
 20. Zhu, Y., Zeng, W., Sun, Y., Feng, F. and Zhou, Y., “Artificial neural network approach to predict the flow stress in the isothermal compression of as-cast TC21 titanium alloy”, *Comput. Mater. Sci.*, 50, 2011, 1785–1790.
 21. Liu, J., Zeng, W., Zhu, Y., Yu, H. and Zhao, Y., “Hot Deformation behavior and flow stress prediction of TC4-DT alloy in single-phase region and dual-phase regions”, *J. Mater. Eng. Perform.*, 24, 2015, 2140–2150.
 22. Mandal, S., Sivaprasad, P. V., Venugopal, S. and Murthy, K. P. N., “Constitutive flow behaviour of austenitic stainless steels under hot deformation: artificial neural network modelling to understand, evaluate and predict”, *Modell. Simul. Mater. Sci. Eng.*, 14, 2006, 334–342.
 23. Rakhshkhorshid, M. and Hashemi, S. H., “Experimental study of hot deformation behavior in API X65 steel”, *Mater. Sci. Eng., A* 573, 2013, 37–44.
 24. Shaban, M. and Eghbali, B., “Determination of critical conditions for dynamic recrystallization of a microalloyed steel”, *Mater. Sci. Eng., A* 527, 2010, 4320–4325.